ELSEVIER

Fire and post-fire management alters soil microbial abundance and activity: A case study in semi-arid shrubland soils

George Vourlitis [a,*], Dylan Steinecke [a], Tanairi Martinez [a], Karen Konda [a], Roxana Rendon [a], Victoria Hall [a], Sherryca Khor [a], Arun Sethuraman [a,b]

[a] Department of Biological Sciences, California State University, San Marcos, CA 92096, United States of America
[b] Department of Biology, San Diego State University, San Diego CA 92182, United States of America

ABSTRACT

Soil microbial communities play a key role in ecological processes; however, the effects of fire, and post-fire management practices such as hydroseeding, on microbial abundance and activity are still poorly known. We sampled surface soil (0–10 cm) from unburned (UNB), burned and naturally regenerating (NAT), and burned but hydroseeded (HYD) chaparral stands on the campus of California State University San Marcos five years after fire. Soil was analyzed for microbial biomass carbon (C), bacterial taxonomic composition at the phylum level, and microbial activity (enzyme activity and nitrification) to test the hypothesis that fire and hydroseeding would significantly alter microbial abundance and activity. Total soil nitrogen (N) and C, microbial C, enzyme activity, and nitrification rate were significantly lower in burned stands than in the UNB stand; however, some of these patterns were affected by hydroseeding. Carbon inputs from hydroseeding, and associated changes in the composition of colonizing plant species, caused soil C and N and microbial C to be similar in the HYD and UNB stands. Relative abundances of bacterial taxa were similar for the UNB, HYD, and NAT stands, and there were no significant differences in taxonomic diversity between the stands. Activities of key C (β-glucosidase, peroxidase) and nutrient (*N*-acetylglucosaminidase (NAGase), phosphatase) cycling enzymes were significantly lower in burned stands, but hydroseeding did not affect their activities, and the declines in enzyme activity were due in part to declines in microbial biomass, soil C and N pools, and increases in pH. Our data suggest that fire and post-fire treatments alter soil microbial biomass and activity for years after fire, which will affect ecosystem C and N cycling and management of fire-prone semi-arid shrublands like chaparral.

1. Introduction

Fire is a common disturbance in many terrestrial ecosystems, especially those that experience high temperature, frequent drought, and long-term fuel buildup (Minnich and Bahre, 1995; Keeley and Brennan, 2012). This is especially true in Mediterranean-climate regions, where population growth and expansion (Venevsky et al., 2002; Marlon et al., 2008), policies of fire suppression (Minnich and Bahre, 1995), and warming and drying associated with climate change (Cayan et al., 2010; Diffenbaugh et al., 2015) are altering fire regimes in already fire-prone woodlands (Running, 2006; Hoover et al., 2019; Lavorel et al., 2020). Depending on fire severity (DeBano and Conrad, 1978), losses of aboveground biomass and surface litter cause both short- (months-years) and long-term (years-decades) changes in ecosystem C and N storage (Wan et al., 2001; Certini, 2005; Kaye et al., 2010; Nave et al.,

2011; Vourlitis and Hentz, 2016; Moya et al., 2018; Pellegrini et al., 2018). Aboveground C and N stocks accumulate over time, often reaching pre-fire levels within the first decade of recovery (Black, 1987; Kaye et al., 2010; Vourlitis and Hentz, 2016; Vourlitis et al., 2021a). Belowground C and nutrient losses tend to be lower than aboveground losses because soil is a poor conductor of heat (Odion and Davis, 2000). Even so, losses of surface organic matter are substantial (Odion and Davis, 2000; Nave et al., 2011), and these losses, coupled with losses of aboveground biomass, affect belowground biomass and soil C and nutrient pools (Kaye et al., 2010; Martí-Roura et al., 2011; Moya et al., 2018; Pellegrini et al., 2018).

Fire-induced changes in above- and belowground C and nutrient stocks have the potential to alter microbial abundance and activity (Barreiro et al., 2015; Barcenas-Moreno et al., 2016; Pressler et al., 2018; Moya et al., 2019). Microbial populations typically decline after fire

(Hart et al., 2005; Dooley and Treseder, 2012; Fontúrbel et al., 2012; Hanan et al., 2016); however, these results may not be universal (Rutigliano et al., 2007) and may depend on fire severity (Bonanomi et al., 2016; Holden et al., 2016; Pressler et al., 2018; Moya et al., 2019), vegetation type (Barcenas-Moreno et al., 2016), and changes in soil environmental characteristics, namely pH, N availability, and C quantity and quality (Tas et al., 2014; Sun et al., 2016). Microbial populations generally increase over time since fire as litter pools increase from shrub recovery, but inhibitory effects of fire can persist for several years (Hart et al., 2005; Knicker, 2007; Fontúrbel et al., 2012). Fire also affects microbial community composition, reportedly causing both short- and long-term declines in microbial diversity (Barreiro et al., 2015; Sun et al., 2016). Studies from Mediterranean ecosystems indicate that fire negatively affects fungi but can stimulate bacteria (Rutigliano et al., 2007; Barreiro et al., 2015). However, declines in fungal biomass may be a function of fire severity, as hotter fires cause charred litter to become relatively more enriched in recalcitrant C due to higher losses of labile C (Bonanomi et al., 2016). Microbial diversity is also affected by the vegetation that colonizes after fire because of its impact on soil C and nutrient stocks (Knelman et al., 2015). Changes in microbial abundance and/or species composition also cause changes in microbial activity. For example, declines in glucosidase and urease activity in post-fire Mediterranean soils persisted up to 1 year after fire (Barreiro et al., 2010; Moya et al., 2018, 2019).

While fire alters soil C and nutrient cycling of semi-arid woodlands, post-fire management strategies can also affect the recovery of plant and soil microbial populations. Land managers may resort to hydroseeding or hydromulching on recently burned chaparral slopes to increase the rate of vegetation recovery and reduce the potential for erosion, C and nutrient loss, and declines in stream water quality (Keeler-Wolf, 1995; Beyers, 2004; Hubbert et al., 2012). Hydroseeding consists of a mixture of seeds, water, nutrients, and organic matter that is applied to the burned area to hasten vegetation development (Asche and Barton, 1995; Keeler-Wolf, 1995; Beyers, 2004), while hydromulching consists of applying organic matter without an artificial seed source (Hubbert et al., 2012). These mixtures often include a C- or nutrient-rich matrix to reduce erosion and improve nutrient and water retention for naturally or artificially germinating seeds (Zink and Allen, 1998; Garcia-Palacios et al., 2010; Oliveira et al., 2014; Busnardo et al., 2017). Hydroseeding is controversial because it can introduce non-native plant species, which can cause a decline plant community diversity and delay native plant recovery (Asche and Barton, 1995; Keeler-Wolf, 1995; Beyers, 2004; Vourlitis et al., 2017). Furthermore, because post-fire seeding and mulching treatments are often amended with C (wood fiber and/or C-rich "tackifiers") and fertilizers, they can have important effects on microbial abundance and diversity, at least early during post-fire succession (Fontúrbel et al., 2012; Barreiro et al., 2016; Vourlitis et al., 2017). However, long-term impacts of post-fire management on microbial abundance, activity, and community composition are not well understood.

We studied burned and unburned chaparral stands on the campus of California State University-San Marcos (CSUSM) to assess the effect of fire and post-fire management on ecosystem C and N cycling and microbial abundance, composition, and activity. One stand had not experienced fire for over 4 decades (unburned), while two adjacent stands burned during the 2014 "Cocos" fire, one of which is recovering naturally and another that was hydroseeded approximately 7 months after fire. Because the fire, and subsequent post-fire treatment was a chance event, these stands were not replicated, which has the potential to add uncertainty to our understanding of how fire and post-fire management affect microbial activity and taxonomic composition. However, the stands are located close to each other, have the same soil type and parent material, and have similar slope and slope aspect. Soil samples were analyzed for physical and chemical properties, microbial activity was assessed by N mineralization and enzyme assays, and bacterial abundance and composition were analyzed using DNA metabarcoding. Given

that fire can alter microbial abundance and function (Dooley and Treseder, 2012; Hanan et al., 2016; Pressler et al., 2018), we hypothesized that the burned stands would have lower microbial abundance and activity than the unburned stand after five years of post-fire recovery. We also hypothesized that hydroseeding would cause significant changes in microbial abundance and activity because hydroseeding alters soil properties and plant recovery (Vourlitis et al., 2017).

2. Methods

2.1. Site description and field sampling design

Soil was sampled in February 2019 from unburned (UNB), burned and naturally recovering (NAT), and a burned and hydroseeded (HYD) chaparral stands located on the campus of California State University San Marcos (CSUSM; 33°07′46″N; 117°09′35″W; Fig. 1). Each stand had eight, 2 m radius (12.65 m^2) circular plots that were randomly located within a ca. 150 m × 50 m area centered within each site, and each plot was separated by at least 10–20 m. Plots on the NAT and HYD stands were installed in March 2015, while plots in the UNB stand were installed in February 2019. All stands have similar underlying granitic parent material, soil type (Typic Xerorthents, Entisol; Bowman et al., 1973), and texture (coarse sandy-loam soil of the Cieneba series, with an average bulk density of 1.34 g/cm^3; Vourlitis et al., 2015). Sites were separated by a maximum distance of 500 m and were located on a NW facing slope at an elevation of 220 m above sea level and an average slope angle of 15°. Average annual temperature and precipitation for the closest long-term measurement site (San Pasqual RAWS; 33°05′29″N; 117°00′44″W; 225 m asl), located 14.3 km SSE of CSUSM were 16.6 °C and 321 mm, respectively, with nearly all of the precipitation (94%) arriving between the months of October and April (https://wrcc.dri.edu/cgi-bin/rawMAIN.pl?caCSPQ; accessed 19 July 2021). Average annual precipitation was 336 mm during the five-year fire recovery period from May 2014 to May 2019, or about 15 mm higher than the long-term average.

NAT and HYD stands were burned during the May 2014 Cocos Fire and were approximately 5 years post fire at the time of field sampling. Both stands were almost completely denuded by the fire, leaving only charred skeletons of the largest shrubs (Fig. 1). While fire intensity was not quantified, the consumption of the tall, dense chaparral vegetation suggests that the fire was severe. Pre-fire vegetation was not quantitatively sampled in the NAT and HYD sites; however, sites were only separated by a small distance (<500 m), and a similar slope aspect, angle, and substrate type suggests that all three sites had similar vegetation prior to fire. Qualitative observations before the fire indicated that pre-fire vegetation was a Chamise-Black Sage series chaparral (Sawyer and Keeler-Wolf, 1995), with *Adenostoma fasciculatum* Hook & Arn., *Salvia mellifera* Green, *Xylococcus bicolor* Nutt., *Rhus integrifolia* (Nutt.) Brewer & *S. Watson* and *Malosma laurina* (Nutt.) Abrams as the dominant woody shrub species, which is consistent with the vegetation of the UNB stand sampled here (Supplemental Table S1). Burned sites also had high coverage of *Ceanothus tomentosus* Parry after fire, which was absent from the unburned site (Supplemental Table S1).

The hydroseeded stand was sprayed approximately 7 months post-fire with a mixture of native chaparral and coastal sage scrub species (Supplemental Table S1). The hydroseed matrix contained 3363 kg/ha of wood fiber and 112 kg/ha of "SpecTack" (Mat, Inc., Floodwood, MN, USA), which is an organic "tackifier" made of a polysaccharide matrix that binds wood fiber and seeds into a slurry. According to the manufacturer, SpecTack is composed of a Guar Gum hydro-colloid polymer that is "non-toxic to all living things." According to personnel that applied the hydroseed mix to the study site, the matrix composition is typical of those used on post-fire hillslopes in southern California (R. McGann, HydroPlant Hydroseeding, Inc. pers. comm.). Plant species in the seed mix (and their seed densities in parentheses) included *Artemisia californica* Less. (2.2 kg/ha), *E. fasciculatum* (5.6 kg/ha), *Acmispon glaber*
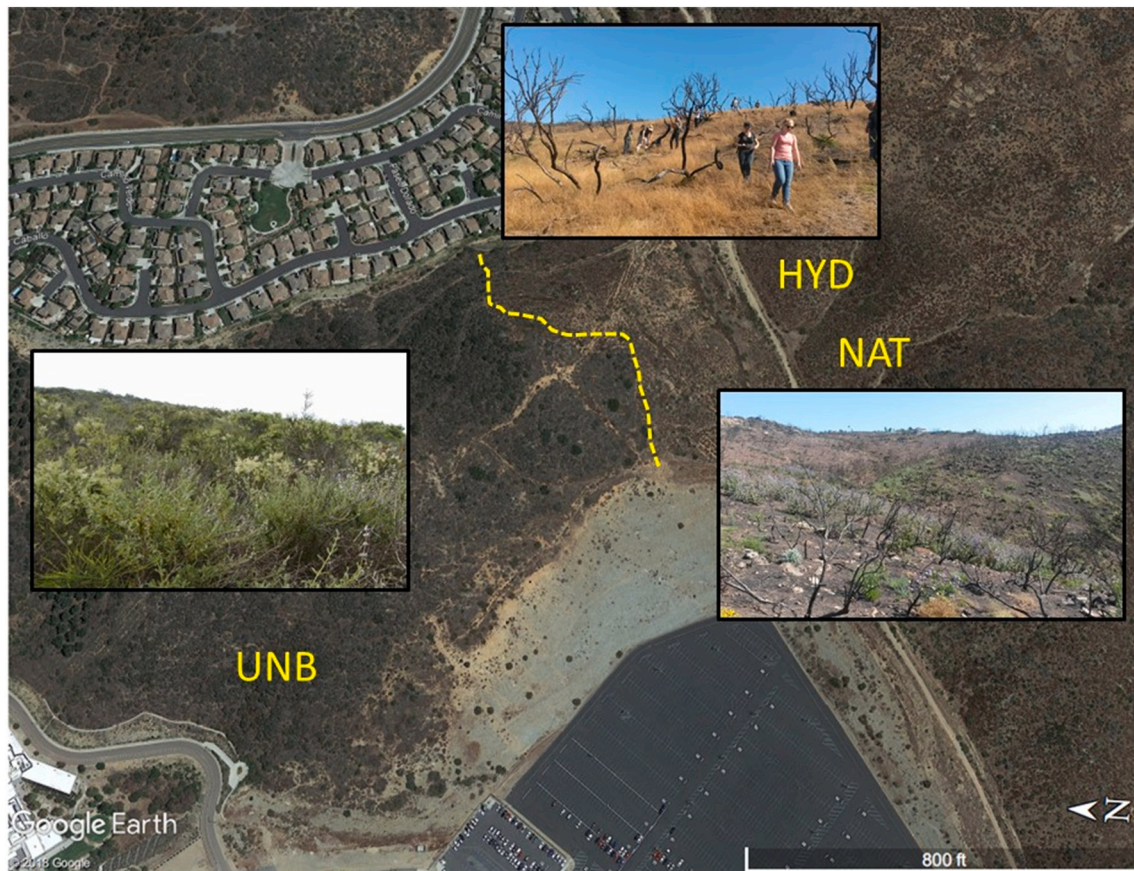
Fig. 1. Google earth image of the approximate locations of the unburned (UNB), burned and hydroseeded (HYD), and burned and naturally recovering (NAT) research sites at California State University San Marcos (CSUSM). The photos from the HYD and NAT sites were taken approximately 2 years post fire while the photo for the UNB site was taken in 2019. The yellow dashed line is the approximate border of the fire. The Google Earth Image was from 2018 and was acquired in September 2019.

(Vogel) Brouilet (6.7 kg/ha), *Mimulus aurantiacus* var. *puniceus* (Nutt.) D. M. Thomps. (2.2 kg/ha), *Isocoma menziesii* (Hook & Arn.) G. Nesom (2.2 kg/ha), *Lupinus succulentus* Koch (3.4 kg/ha), *Festuca microstachys* (Nutt.) Benth. (6.7 kg/ha), and *Bromus carinatus* Hook & Arn (11.2 kg/ha) (Supplemental Table S1).

2.2. Field measurements

Soil samples were obtained from each plot at each site in February 2019 from the upper 0–10 cm soil layer using a 5 cm diameter and 15 cm height PVC corer. This sampling depth was chosen because it has the highest soil organic C stocks and is heavily influenced by the type and amount of vegetation (Jobbagy and Jackson, 2000); however, we acknowledge that the effects of fire may be small at a soil depth of 10 cm because soil is a poor conductor of heat (Odion and Davis, 2000). A total of 3-subsamples were randomly taken from each plot to capture the small-scale (<m) variation in plant cover (n = 3 sub-samples/plot, 8 plots/stand, 24 subsamples/stand, 72 subsamples total). Each sample was stored in an individual sterile "Whirl-Pak" bag, and samples were immediately sieved with a 2 mm sieve to remove debris and stored in a refrigerator at 4 °C for 1 week (Boone et al., 1999). A portion of each sub-sample was combined to yield one composite sample for each plot (n = 8 composite samples/stand) that was used for all soil physical and chemical analyses (Section 2.3), microbial biomass C (Section 2.4), and extracellular enzyme activity (Section 2.6).

Vegetation abundance was measured in March 2015 and September 2018 in the NAT and HYD stands and in March 2019 in all stands, which was about 1 week after collection of soil samples. Measurements were made in 2 m radius (12.56 m^2) circular plots that were randomly located in each stand (n = 10 plots/stand in 2015 and 2018) and in the same 12.56 m^2 plots where soil samples were taken in 2019 (8 plots/stand). All woody shrubs rooted within each circular plot were identified to species, counted, and measured for canopy area (A) = $\pi D^2/4$, where D was the average shrub diameter calculated from measurements of the maximum and perpendicular diameter (Vourlitis et al., 2017). Density was calculated as the number of individuals of each species divided by plot area and percent woody shrub cover was calculated as the total canopy area divided by the area of the plot ($\times 100$). Shrub species richness was calculated as the number of species per plot. Cover of herbaceous plants was measured in four-0.5 × 0.5 m (0.25 m^2) gridded-quadrats centered in each plot (n = 8 plots/stand) using a point-intercept method (Jonasson, 1988). Each quadrat was separated into 25 sub-quadrats, and the number of times herbaceous plants were "hit" by grid intercepts were counted. Percent herbaceous cover was calculated as the number of "hits" divided by the total number of possible intercepts in each quadrat ($\times 100$).

2.3. Laboratory sample analyses

Composite soil samples were analyzed for pH, soil moisture, extractable N (NH$_4$ + NO$_3$), and total N and C. Soil pH was measured in 2:1 DI-water:soil extracts using a standard pH electrode. For extractable N, 10 g of the fresh soil sample was extracted in 40 ml of 0.5M K$_2$SO$_4$ to quantify soil extractable NH$_4$ and NO$_3$ using the salicylate (Mulvaney, 1996) and vanadium chloride (Miranda et al., 2001) methods, respectively. Absorbance was read at 667 nm (NH$_4$) and 540 nm (NO$_3$) using a

spectrophotometer, and absorbance was converted to NH_4 and NO_3 concentration (mgN/kg dry soil) using a standard curve. Another portion of the soil sample was dried at 105 °C until constant weight. Gravimetric soil moisture was calculated as the difference in fresh and oven-dry soil mass divided by the dry soil mass. Oven-dried soil was ground using a ball mill (MM200, Retsch, Düsseldorf, Germany) for measurements of total N and C by dry combustion (ECS 4010, Costech Analytical Technologies, Inc., Valencia, CA, USA).

2.4. Measurements of microbial abundance

Composite soil samples were analyzed for microbial biomass using the chloroform fumigation and extraction method (Brookes et al., 1985). Duplicate 10 g samples were weighed into 50 ml beakers, one of which was fumigated with chloroform for a period of 5 days and another that was unfumigated. Both fumigated and unfumigated samples were extracted with 0.5M K_2SO_4, which was analyzed for dissolved C by absorption at 600 nm using a modified version of the Walkley-Black method (Sims and Haby, 1971). The difference in absorption between the fumigated and un-fumigated samples was taken as the microbial C content based on a standard curve generated from glucose (Brookes et al., 1985).

2.5. DNA metabarcoding

Genomic DNA was extracted from all 72 sub-samples using the ZymoBIOMICS™ DNA MicroPrep Kit. DNA quality and quantity were analyzed using gel electrophoresis, a nanodrop spectrophotometer, and a Qubit Fluorometer. Extracted DNA was then amplified using 16s rRNA primers for the V3–V4 region (~460 bp, ~596 bp upon addition of barcoded primers, proprietary to Zymo Research: D6405-2-400) ligated with Illumina adapters to amplify ~500–600 base pairs from each sample. An equal concentration of amplified DNA from each of the plot sub-samples was then combined to create one composite DNA sample for each plot/site (n = 8 plots/site × 3 sites = 24 total composite bacterial DNA samples). Unfortunately, errors during compositing led to contamination for two of the plot samples from the HYD site, causing the number of composite samples to be eight for the NAT and UNB sites and six for the HYD site. These DNA samples were stored at −80 °C until all samples were processed.

Libraries were then uniquely barcoded using Illumina Nextera® XT indices, cleaned using Agencourt AMPure XP magnetic beads, analyzed on an Agilent Bioanalyzer, and sequenced on an Illumina MiSeq (150 bp, paired end) at the UC Riverside Genomics Core Facility. Raw sequence data was demultiplexed based on their unique indices, quality controlled to trim reads below Q20, mapped back to the SILVA database (Quast et al., 2013), and then analyzed using the MOTHUR pipeline (Schloss et al., 2009) on The Galaxy Project (Afgan et al., 2018). Briefly, paired-end reads (150 bp) were assembled into contigs, followed by filtering of short contigs (<400 bp), discarding duplicated contigs within samples, and standardizing for differences in sequencing depth across samples. These contigs (and their reverse complements) were then aligned to the SILVA V4 database (Quast et al., 2013) using a kmer size of 8 with the Needleman-Wunsch algorithm. Misalignments and chimeric sequences were trimmed outside of the V3-V4 region, and data were then clustered into OTU's based on the Ribosomal Database Project taxonomy (Cole et al., 2013). Bacterial sequence data was of very high quality (Illumina on-line support), with nearly 90% barcode match, 91% of bases with a quality (Q-score) > 30, and a mean quality of score of 35.83.

2.6. Measurements of microbial activity

Composite soil samples were analyzed for the enzyme activities of β-glucosidase, N-acetylglucosaminidase (NAGase), and phosphatase according to Jackson et al. (2013) and peroxidase (Vourlitis et al., 2021b). For all enzyme assays, 5 g of fresh soil was weighed from each

plot into sterile plastic tubes containing 5 ml of 50 mM acetate buffer that was pH adjusted to 5.0–5.5. The soil-buffer solution was mixed using a vortex mixer (Genie 2, Thermo-Fisher Scientific, Hampton, NH) and incubated at room temperature for 24 h. After incubation, 150 μl of soil slurry was transferred to a 96-well plate with 150 μl of the corresponding p-nitrophenyl (pNP)-linked substrate, which was 5 mM pNP-phosphate for phosphatase, 5 mM pNP-β-glucopyranoside for β-glucosidase, and 5 mM pNP-β-acetylglucosamide for NAGase (Jackson et al., 2013). Blanks consisted of buffer solutions, and standards ranging from 0 to 0.85 mM concentrations were made using the appropriate pNP-linked substrates and acetate buffer. Plates incubated at room temperature for 1–5 h depending on the enzyme, and the reaction was stopped by adding 10 μl of NaOH and 190 μl of distilled water. Samples were run in triplicate, while blanks and standards were run in duplicate. Absorbance was read at 410 nm using a microplate reader (EPOCH 2, Biotek, Inc., Winooski, VT).

Peroxidase activity was measured by absorbance using L-3,4-dihydroxyphenylalanine (L-DOPA) as the substrate (Vourlitis et al., 2021b). The soil-buffer mixture was thoroughly mixed, and 150 μl of soil slurry was combined with 50 μl of 25 mM L-DOPA and 10 μl of 0.3% H_2O_2 in a 96-well plate. Blanks consisted of buffer solution only, and standards ranging from 0 to 0.85 mM concentrations were prepared from the L-DOPA, H_2O_2, and acetate buffer. Samples, blanks, and standards were covered with aluminum foil and incubated for 5 h, and absorbance was read at 450 nM using a microplate reader (EPOCH 2, Biotek, Inc., Winooski, VT).

Enzyme activity (E_a; nmol g dry soil^{-1} h^{-1}) was calculated as $E_a = A_{adj} \times C / M \times t$, where A_{adj} = the adjusted absorbance (sample absorbance − blank absorbance), C = pNP-linked or L-DOPA substrate concentration per unit absorbance determined from the standard curve, M = the mass of air-dried soil (5 g) corrected for soil moisture, and t = incubation time.

Rates of net nitrification were analyzed using a 1-week laboratory incubation. Fresh, composite soil samples were weighed in duplicate, which 10 g was immediately extracted for NO_3 in 0.5M K_2SO_4 (described above) and another 10 g soil sample incubated for 7 days in the dark at a temperature of 25 °C and a gravimetric soil moisture of 25%. After incubation, the soil sample was extracted for NO_3 in 0.5M K_2SO_4 and both incubated and un-incubated extracts were analyzed for NO_3 (as described above) by absorbance at a wavelength of 540 nm using a spectrophotometer (Miranda et al., 2001). Net nitrification rate was calculated as the incubated – un-incubated NO_3 concentration divided by the elapsed time of the incubation. Unfortunately, rates of net N mineralization (NH_4 + NO_3) could not be quantified because post-incubation samples of NH_4 were contaminated and had to be discarded. Thus, only nitrification rate is reported here. However, nitrification rates are rapid in chaparral soils and most of the extractable N is in the form of NO_3 (Vourlitis and Zorba, 2007).

2.7. Statistical analyses

Principle Components Analysis (PCA) was used to assess variations in soil properties, vegetation characteristic, and microbial activity, and microbial community composition, between the different stands. Varimax rotation was used to generate factors from the input variables (see Supplemental Table 2) and factors with eigenvalues >1 were retained (Kaiser, 1960).

Redundancy analysis (RDA) was used to link variations in microbial activity and taxonomic relative abundance to variations in soil (soil moisture, extractable N, pH, and total N and C) and vegetation (shrub and herbaceous cover, shrub density, and shrub species richness) properties between the different plots.

Differences in vegetation attributes, soil variables, and microbial activity were analyzed using one-way ANOVA followed by a Tukey-Kramer post-hoc test if the ANOVA was statistically significant (p < 0.05). Sites were treated as random factors and data were tested for

normality and heteroscedasticity, and data violating these assumptions were LN-transformed.

A repeated-measures ANOVA was used to analyze changes in woody and herbaceous species cover in the NAT and HYD plots over time because these plots were sampled on three different sampling dates. For these analyses, sites were considered random factors and time was considered a fixed factor. Assumptions of equality and compound-symmetry (sphericity), respectively ($p \leq 0.10$) of the between-group covariance matrices were tested using Box's M and Mauchly's tests, respectively, and Geisser-Greenhouse p-values were calculated for interactions when these assumptions were violated.

Because DNA sample contamination led to an unbalanced design, differences in relative abundance and diversity of bacterial phyla between the UNB, HYD, and NAT sites were assessed using bootstrap randomization techniques (Efron and Tibshirani, 1993). For relative abundance the bootstrap randomly sampled (with replacement) the relative abundance of a given phylum from each plot per site over 1000 iterations and calculated the grand mean and a ±95% confidence interval for each site. Relative abundance for a given phylum was assumed to be statistically significant ($p < 0.05$) if there was no overlap in the ±95% confidence intervals (Efron and Tibshirani, 1993). Bacterial phylum diversity was calculated from relative abundance using the

Shannon Weiner H', where $H' = -\Sigma [p_i \times LN(p_i)]$, where p_i is the relative abundance of phylum p in plot i and $LN(p_i)$ is the natural log of p_i (Magurran, 1988). In turn, H' was bootstrapped for each site by randomly sampling (with replacement) the relative abundance of all bacterial phyla and calculating H'. The bootstrapped H' was then recalculated over 1000 iterations, and the mean (±95% confidence interval) for each site was calculated. As with the relative abundance data, bootstrapped H' for each site was assumed to be statistically significant ($p < 0.05$) if there was no overlap in the ±95% confidence intervals (Efron and Tibshirani, 1993).

PCA and ANOVA analyses (one-way and repeated measures) were conducted using NCSS 12 Statistical Software (NCSS, LLC. Kaysville, Utah, USA, ncss.com/software/ncss). Bootstrapping was conducted using NS Excel (Christie, 2004). RDA was conducted using the Vegan package in R (version 4.0.5).

3. Results

3.1. Environmental characteristics

PCA explained 84% of the variance in soil properties between the different sites, with PCA axis 1 (PCA1) explaining 53% and PCA2
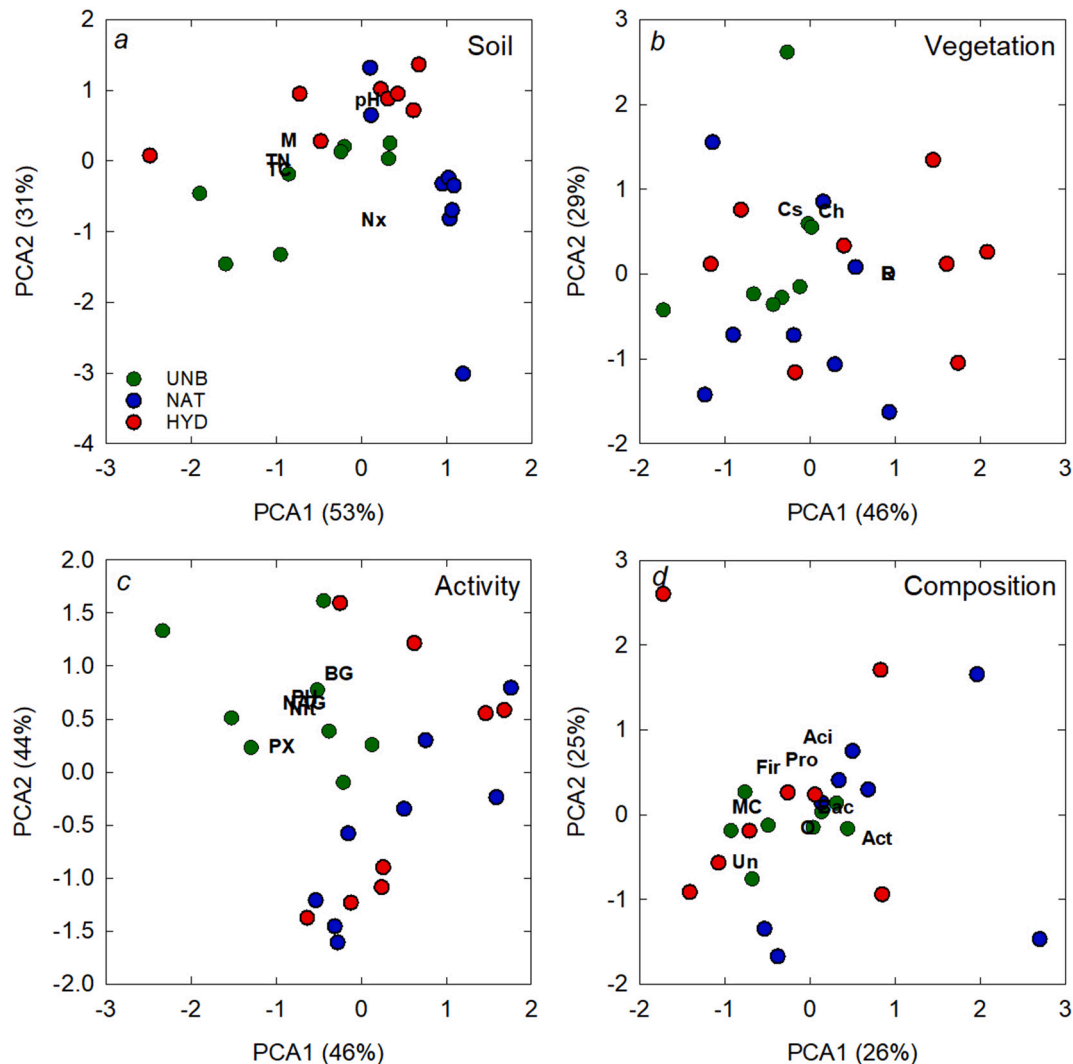

Fig. 2. Principle components analysis (PCA) of the soil (a), vegetation (b), microbial activity (c), and microbial taxonomic composition (d) properties associated with the unburned (green-symbols), naturally regenerating (blue-symbols), and hydroseeded (red-symbols) stands measured in spring 2019. The amount of variance explained by each PCA axis (%) is displayed in each panel. The loading values for each factor (bold text) are overlaid on each panel. Variables used in the PCA are shown in Supplemental table 2.

explaining an additional 31% (Fig. 2a). PCA1 was negatively correlated with soil organic C (SOC) while PCA2 was positively correlated with pH and negatively correlated with extractable N (Supplemental Table 2). Unburned (UNB) and hydroseeded (HYD) plots appeared to be separated more strongly by PCA1, while the naturally regenerating (NAT) plots appeared to be dispersed more by PCA2 than PCA 1 (Fig. 2a). Almost all of the UNB plots, and approximately half of the HYD plots, were clustered on the left-hand side of PCA 1, and nearly all of the NAT plots on the right-hand side of PCA1. This implies that the UNB and HYD plots had higher SOC than the NAT plots. Most of the NAT plots, and approximately half of the UNB plots, were in the lower (negative) portion of PCA2, while nearly all of the HYD plots were in the upper (positive) potion of PCA2 (Fig. 2a). This implies that the HYD and UNB plots had higher relatively pH and lower extractable N than the NAT plots.

PCA explained 75% of the overall variance in vegetation attributes, with PCA1 explaining 46% and PCA2 explaining 29% (Fig. 2b). PCA1 was positively correlated with shrub density and species richness while PCA2 was positively correlated with shrub and herbaceous cover (Supplemental Table 2). Most of the UNB plots were bunched in the center-left and lower left quadrant of the plot indicating lower shrub density and species richness than the other plots (Fig. 2b). Most of the HYD plots were arrayed along the upper half and right-hand side of the plot indicating relatively higher shrub and herbaceous cover, shrub density, and/ or higher species richness than the NAT stands (Fig. 2b).

PCA explained 90% of the variability in microbial activity, with PCA1 explaining 46% and PCA2 explaining 44% (Fig. 2c). PCA1 was negatively correlated with all measures of microbial activity, but peroxidase activity appeared to be the dominant variable, while PCA2

was positively correlated with all measures of microbial activity but β-glucosidase activity appeared to be the dominant variable driving PCA2 (Supplemental Table 2). Most of the UNB plots were scattered in the upper left-had quadrant of the scatterplot, indicating higher micorbial activity (Fig. 2c). The NAT and HYD plots were dispersed more along PCA2 than the UNB lots, and on average, the NAT plots appeared to have lower scores than the HYD plots (Fig. 2c) implying and overall lower rate of microbial activity.

The PCA for microbial community composition was less revealing because most of the plots were bunched in the center and lower left-hand quadrant of the plot (Fig. 2d). However, PCA explained 50% of the overall variation in microbial composition (Fig. 2d) with each axis explaining about half of the overall variability (Supplemental Table 2). Axis 1 was negatively correlated with microbial C content and the relative abundance of unclassified bacteria and positively correlated with *Actinobacteria* abundance, while axis 2 was positively correlated with *Acidobacteria* and *Proteobacteria* relative abundance (Supplemental Table 2). All of the UNB plots were bunched toward the middle of the PCA biplot, implying relatively similar microbial composition in the plots, while the NAT, and to a lesser extent, HYD plots exhibited more scatter along both axes (Fig. 2d). Relatively more of the HYD plots were scattered toward the left-hand side of the biplot while more of the NAT plots toward the center and right-hand side of the biplot (Fig. 2d), indicating relatively higher *Actinobacteria*, *Acidobacteria,* and *Proteobacteria* and lower unclassified bacterial abundances for the NAT plots.

Many of the trends seen in the PCA were confirmed by stand-level comparisons. For example, soil pH was similar between the NAT and UNB stands, but the HYD stand had significantly higher pH (Fig. 3a), which explains the consistently positive scores for the HYD plots along
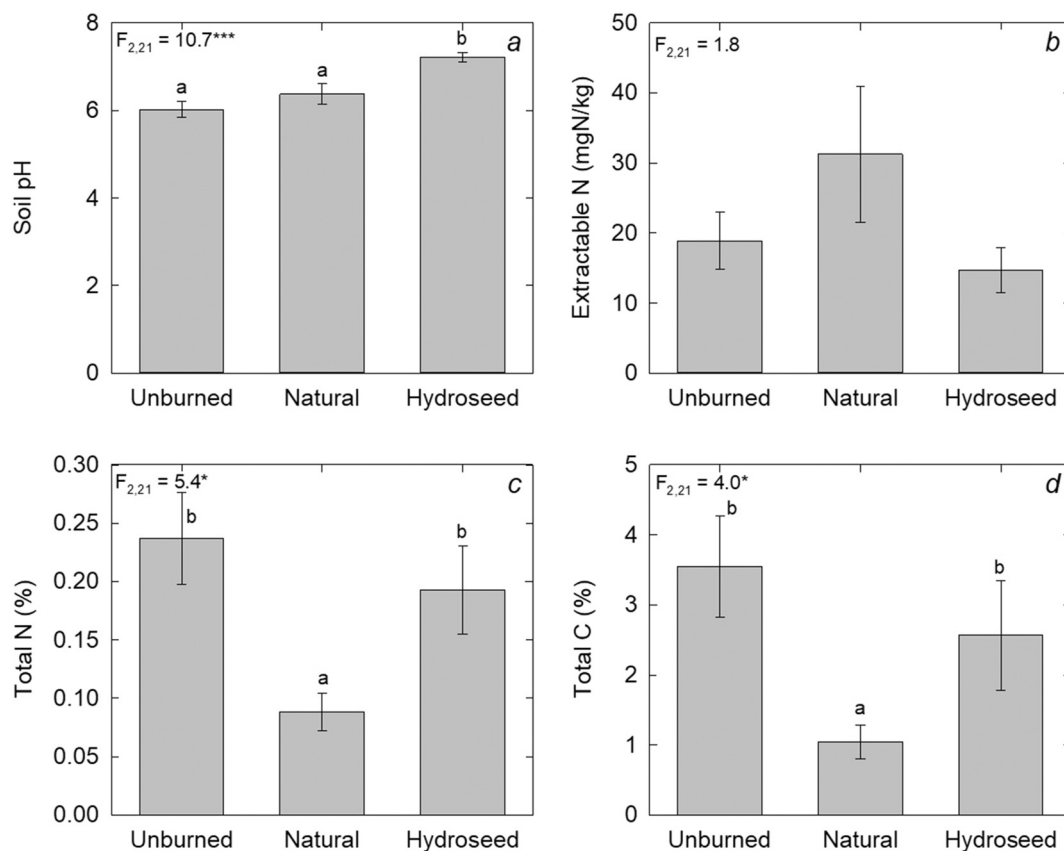

Fig. 3. Mean ($\pm$se; $n = 8$) soil pH (a), extractable nitrogen ($NH_4 + NO_3$) (b), total N (c), and total C (d) for unburned, burned but naturally regenerating (natural), and burned but hydroseeded chaparral stands on the campus of California State University, San Marcos. Results from a 1-way ANOVA (F-statistic and degrees of freedom) are shown; *$p < 0.05$, **$p < 0.01$, ***$p < 0.001$. Means with a different lower-case letter are significantly ($p < 0.05$) different from each other according to a Tukey-Kramer post-hoc test.

the PCA2 axis (Fig. 2a). In contrast, the NAT stand had significantly lower total N (Fig. 3c) and total C (Fig. 3d) than both the HYD and UNB stands, which explains the consistent positive scores for the NAT plots along the PCA1 axis (Fig. 2a). Concentrations of extractable N were not significantly different between the three stands (Fig. 3b).

Variation in shrub and herbaceous cover (Fig. 4a and b) and shrub density (Fig. 4c) were not significantly different between the stands in the spring of 2019, but the HYD stand had considerably higher shrub species richness that the other stands (Fig. 4d). These differences likely explain the relatively higher density of HYD plots on the right-hand side of axis 1 in the vegetation PCA (Fig. 2b).

While vegetation properties in the spring of 2019 were not consistently different between the stands, there were significant differences in the trajectory of vegetation recovery between the burned stands (Fig. 5). Shrub recovery was rapid for both stands but there was no statistically significant difference in total shrub cover over the five-year recovery period (Fig. 5a). However, species composition was markedly different, and with the exception of *Mimulus aurantiacus* and *Xylococcus bicolor*, the dominant shrubs in the HYD stand reflected those species added to the hydroseed mix rather than the species that were re-seeding or re-sprouting in the NAT stand (Supplemental Table S1). Furthermore, the addition of novel (but native) species increased species richness significantly in the HYD plots (Fig. 4d). There also was a significant stand × time interaction for herbaceous cover, which was due to the significantly higher herbaceous cover for HYD plots than NAT plots over most of the post-fire recovery period (Fig. 5b). Thus, while herbaceous cover was not different in between the sites the spring of 2019 (Fig. 4b) the HDY plots had a history of higher herbaceous cover over most of the post-fire period.

3.2. Microbial abundance and composition

Microbial C concentration was highest in the UNB and HYD stands and lowest in the NAT stand (Fig. 6a). This pattern is apparent in the PCA with more of the NAT plots scattered toward the right-hand side of the plot and more of the HYD and UNB plots located toward the left-hand side of the plot (Fig. 2d). However, bacterial diversity at the phylum level was similar between the burned and unburned study sites (Fig. 6b).

The majority of the DNA extracted from all of the sites (29–39%) was not able to be classified by the MOTHUR analyses, but most of the classified sequences were in the phyla *Actinobacteria* and *Proteobacteria*, which made up on average 19 and 27% of the relative abundance, respectively (Fig. 7). Most of the phyla had similar relative abundances in the burned and unburned stands, which was reflected by the close scatter of points in the center of the PCA plot (Fig. 2d). The relative abundance of copiotrophic phyla (*Actinobacteria*, *Bacteroidetes*, *Firmicutes*, and *Proteobacteria*) outnumbered oligotrophic phyla (*Acidobacteria* and "other") by 5:1 (Fig. 7).
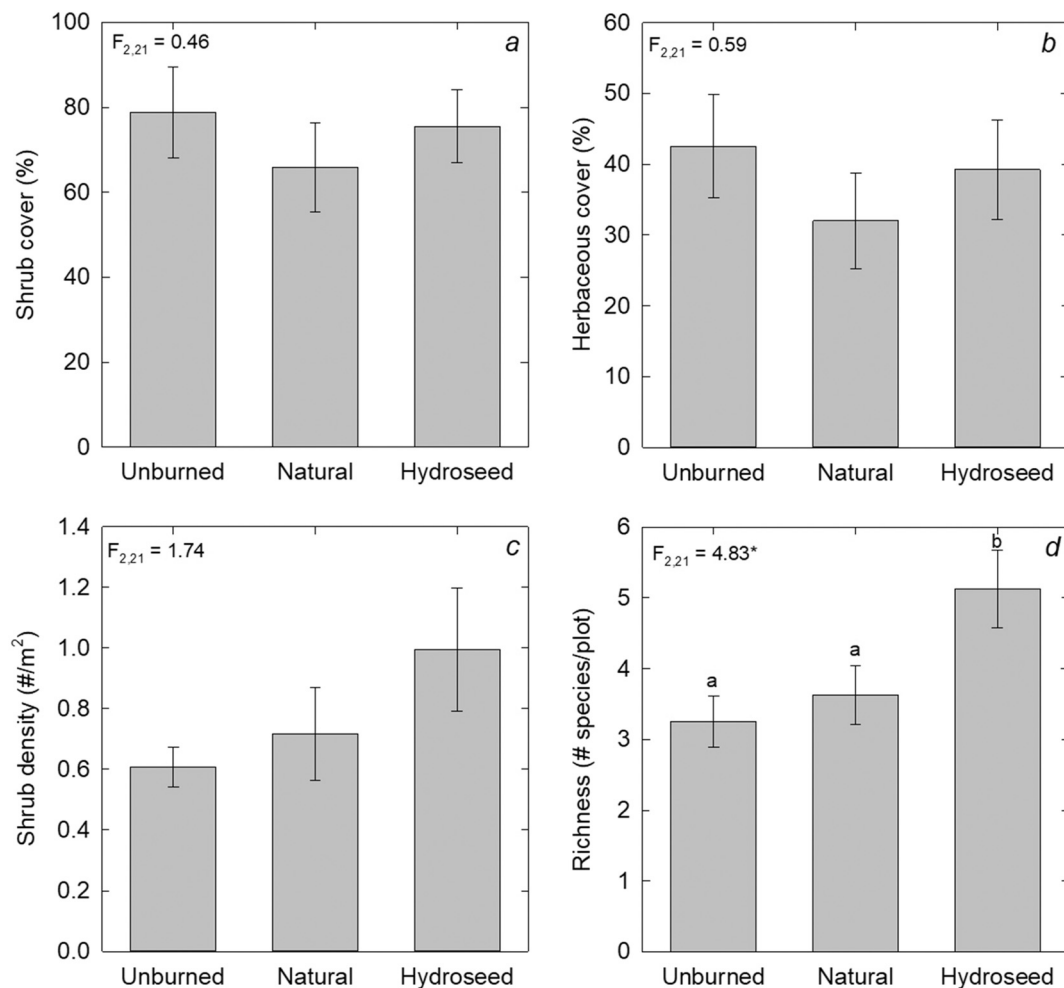

Fig. 4. Mean (±se; $n = 8$ plots/stand) shrub cover (a), herbaceous cover (b), shrub density (c), and shrub species richness (d) for unburned, burned but naturally regenerating (natural), and burned but hydroseeded chaparral stands measured in the spring 2019 on the campus of California State University, San Marcos. Results from a 1-way ANOVA (F-statistic and degrees of freedom) are shown; *$p < 0.05$, **$p < 0.01$, ***$p < 0.001$. Means with a different lower-case letter are significantly ($p < 0.05$) different from each other according to a Tukey-Kramer post-hoc test.
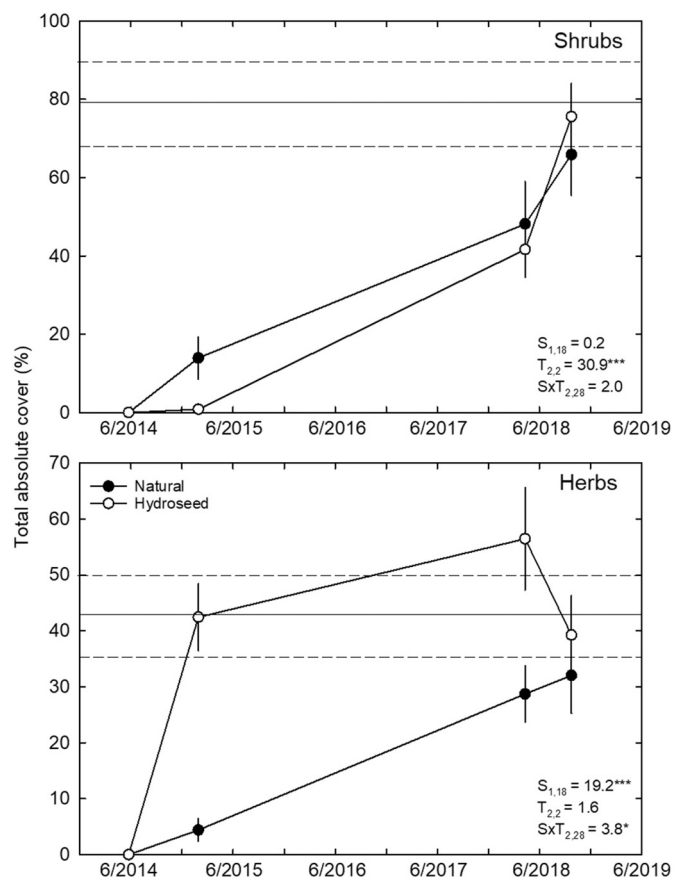
Fig. 5. Mean ($\pm$se; $n = 8$–10) absolute cover for woody shrubs (top-panel) and herbaceous (bottom-panel) plants for naturally recovering (black-symbols) and hydroseeded (white-symbols) chaparral stands on the campus of California State University, San Marcos. Results from a repeated-measures ANOVA (F-statistic and degrees of freedom) are shown for site (S), time (T), and the S × T interaction; *$p < 0.05$, **$p < 0.01$, ***$p < 0.001$. The solid horizontal line in each panel is the mean woody shrub (top-panel) and herbaceous (bottom-panel) cover of the unburned stand measured in March 2019, while the horizontal dashed lines represent the standard error of the mean ($n = 8$).

3.3. Microbial activity

Burned sites had significantly lower rates of enzyme activity than the UNB site, but differences between the NAT and HYD stands were not statistically significant for all measures of microbial activity except nitrification (Fig. 8). Rates of activity for most enzymes were nearly 50% lower for burned areas than in the UNB stand, which was reflected by the higher density of NAT and HYD points on the right-hand side of the PCA plot (Fig. 2c). Nitrification was the only measure of microbial activity that exhibited a significant difference between the NAT and HYD plots, and nitrification rates were on average 6-times higher in HYD plots than in NAT plots (Fig. 8e).

3.4. Environmental controls on microbial activity and relative abundance

Redundancy analysis (RDA) results indicated that β-glucosidase, phosphatase, and NAGase activity scaled positively with spatial variations in total soil C and N and soil moisture and negatively with soil pH (Fig. 9a). As was found with the PCA results (Fig. 2a), total N and C also tended to be higher in UNB plots while pH was highest in HYD plots, which was also supported by ANOVA results (Fig. 3). Pearson correlation analysis further supports this interpretation, as phosphatase, NAGase, and peroxidase were found to be negatively correlated with pH, all measures of microbial activity were positively correlated with soil
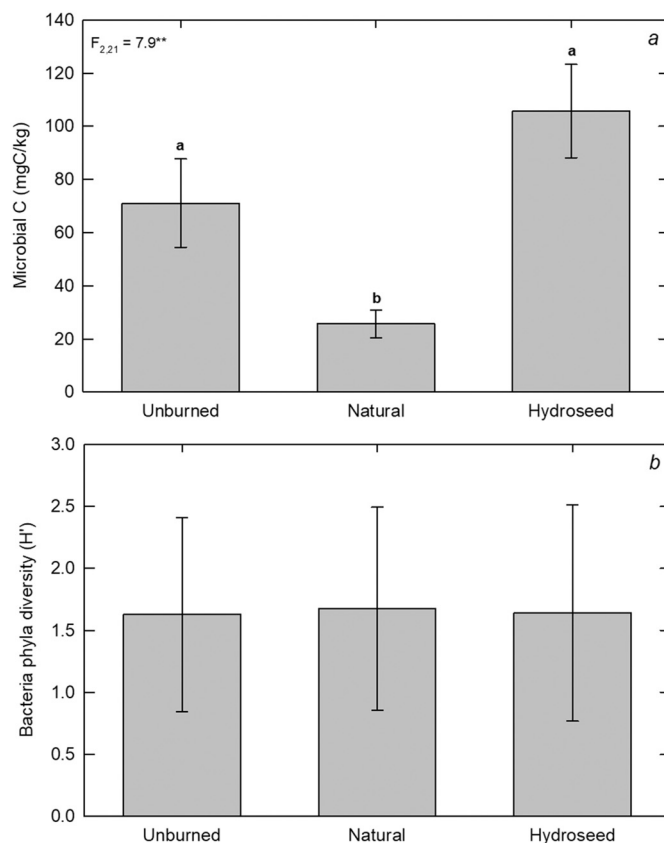

Fig. 6. Mean ($\pm$se; $n = 8$) soil microbial C concentration (a) and the mean ($\pm$95% confidence interval) bacteria phylum diversity (b) from soil samples obtained from unburned, burned but naturally regenerating (natural), and burned but hydroseeded chaparral stands on the campus of California State University, San Marcos. For panel (a) results from a 1-way ANOVA (F-statistic and degrees of freedom) are shown; *$p < 0.05$, **$p < 0.01$, ***$p < 0.001$. Means with a different lower-case letter are significantly ($p < 0.05$) different from each other according to a Tukey-Kramer post-hoc test. For panel (b), phylum diversity was calculated as the Shannon-Weiner H′, and confidence intervals were calculated by bootstrapping H′ values for each site over 1000 iterations.

moisture, and all measures of activity except peroxidase activity were positively correlated with total soil N and C (Supplemental Fig. S1). Vegetation variables appeared to have little influence on microbial activity (Fig. 9a; Supplemental Fig. S1).

Variations extractable N appeared to positively influence the relative abundance of *Actinobacteria* but negatively influence the abundance of *Proteobacteria* and unclassified bacteria (Fig. 9b). These patterns were supported by Pearson correlation analysis (Supplemental Fig. S1). Microbial biomass C was positively related to variations in soil moisture, total N and C, and soil pH, which tended to be higher in UNB (total N, C, and moisture) and HYD (pH) plots (Fig. 2). However, correlation analysis indicated that the main driver of microbial biomass C was extractable N, which was negatively correlated with microbial C (Supplemental Fig. S1). All of the other bacterial taxa scaled toward the middle of the RDA plot, indicating little influence by the soil or vegetation variables studied here. However, correlation analysis indicated that the relative abundance of *Firmicutes* was positively correlated with soil pH (Supplemental Fig. S1).

4. Discussion

4.1. Effects of fire

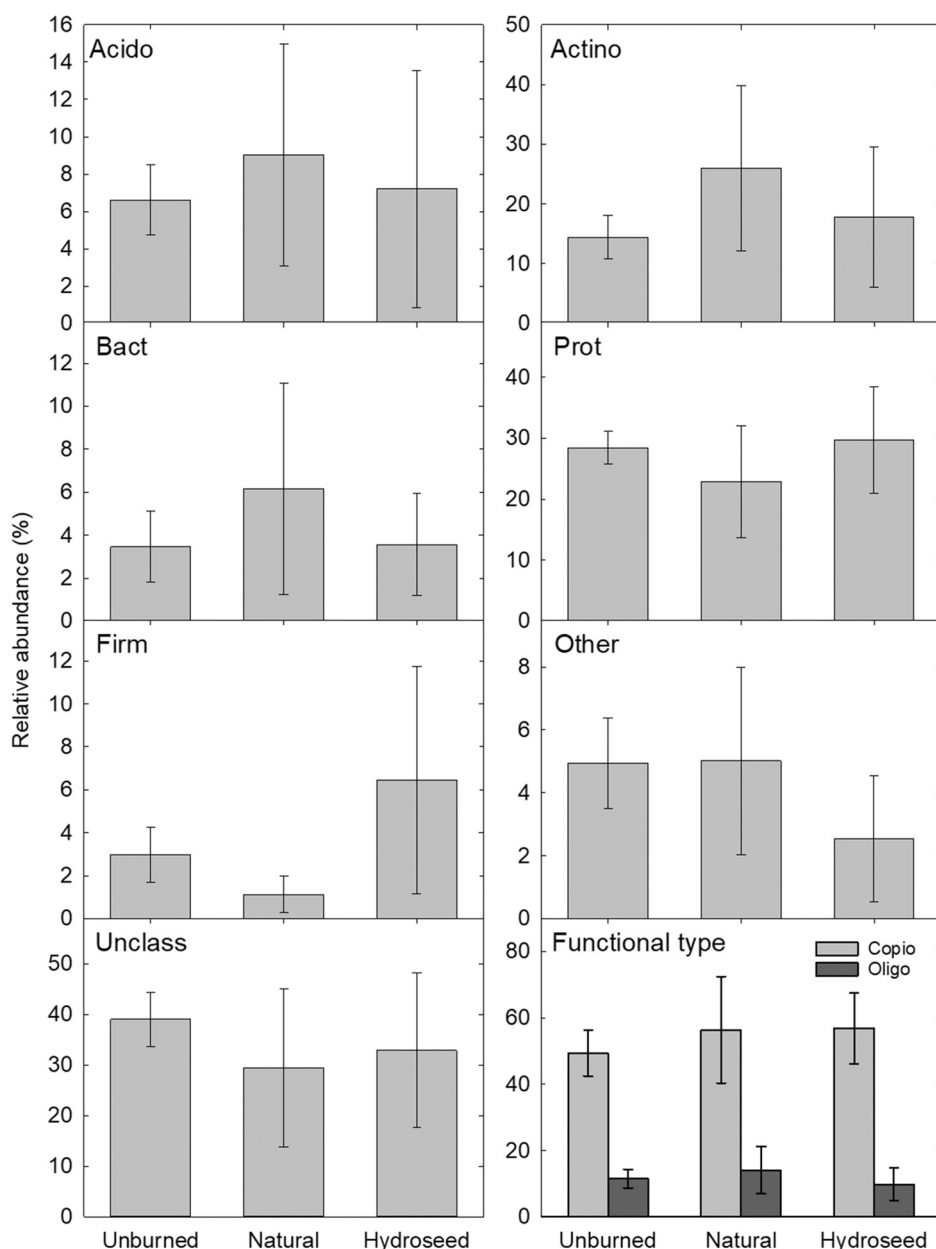The naturally regenerating stand (NAT) had lower total soil N and C,

Fig. 7. Mean (±95% confidence interval) relative abundance of bacteria phyla calculated by bootstrapping over 1000 iterations (see Section 2.5: data analysis). Acido *Acidobacteria*; Actino = *Actinobacteria*; Bact = *Bacteroidetes*; Firm = *Firmicutes*; Prot = *Proteobacteria*; Other = the sum of bacterial phyla with a relative abundance <5% (*Chloroflexi*, *Gemmatimonadetes*, *Nitrospirae*, *Planctomycetes*, and *Verrucomicrobia*); Unclass = unclassified; Functional type = Copiotrophic (light-gray) and Oligotrophic (dark-gray) bacteria.

microbial biomass, enzyme activity, and nitrification rate than the unburned (UNB) stand, thus supporting our initial hypothesis that the burned stands would have lower microbial abundance and activity than the unburned stand after 5 years of post-fire recovery. The lower total soil N and C in the NAT stand implies that the 2014 "Cocos" fire was severe enough to consume some of soil C and N stocks in the upper 10 cm layer (DeBano and Conrad, 1978; Odion and Davis, 2000; Nave et al., 2011). Heat associated with fire can cause high rates of mortality for soil microbes, and while microbial populations may rebound rapidly after fire (Hart et al., 2005; Dooley and Treseder, 2012; Hanan et al., 2016), our data imply that microbial biomass in naturally regenerating plots may still be lower than in unburned chaparral up to 5 years post-fire. However, the relative abundance and diversity of bacterial phyla were similar between the UNB and NAT sites, suggesting that the difference in microbial C between the UNB and NAT sites may have been due to differences in fungal abundance. Fungi are primarily associated with the degradation of recalcitrant organic matter, such as woody debris (Rutigliano et al., 2007; Sinsabaugh et al., 2008; Dooley and Treseder, 2012; Pressler et al., 2018), which was largely consumed in the NAT

stand. While speculative, this interpretation is consistent with observations from other Mediterranean shrublands where fire negatively affected fungi more than bacteria (Rutigliano et al., 2007; Barreiro et al., 2015).

The activity of C (β-glucosidase and peroxidase) and nutrient cycling (NAGase and phosphatase) enzymes was also lower in the NAT stand after 5 years of recovery, which may have been due lower soil C and N pool size or a change in the quality of C and nutrient inputs (Knelman et al., 2017; Ribeiro-Kumara et al., 2020). Indeed, β-glucosidase, NAGase, and phosphatase activity were positively correlated with total soil C and N (Fig. 9a; Supplemental Fig. S1), suggesting that lower soil C and N in the NAT stand was responsible in part for the reductions in extracellular enzyme activity. Similar patterns were observed for nitrification, which is consistent with those reported by Vourlitis et al. (2017) two years post-fire. Low enzyme (urease and phosphatase) activity after 5 years of post-fire recovery has also been observed for burned Mediterranean forests, suggesting that long-term reductions in microbial activity may be common, especially after sever fire (Moya et al., 2018, 2019). Presumably, enzyme activity and nitrification will
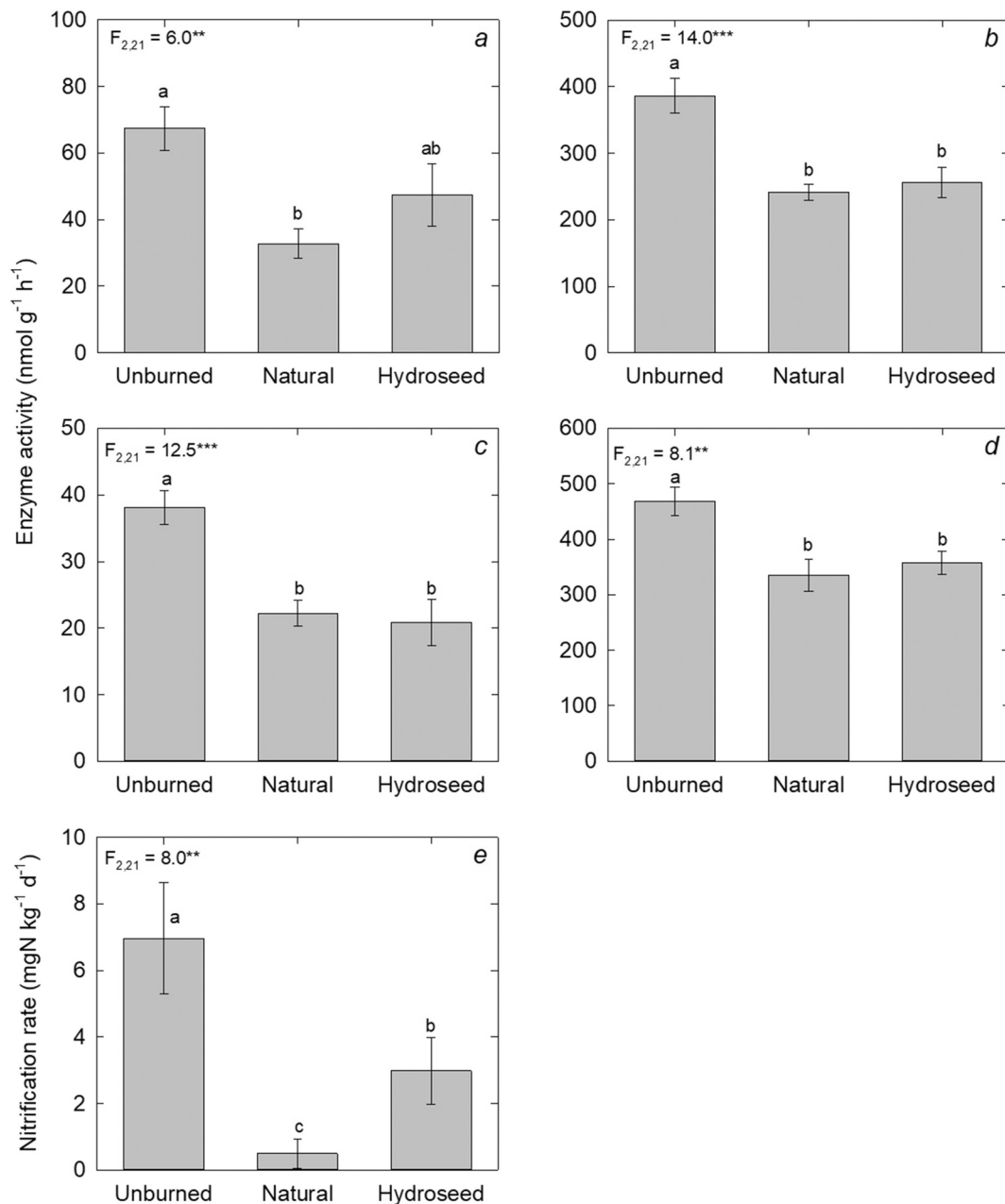
Fig. 8. Mean (±se; n = 8) β-glucosidase (a) phosphatase (b), NAGase (c), and peroxidase (d) activity and net nitrification rate (e) for unburned, burned but naturally regenerating (natural), and burned but hydroseeded (hydroseed) chaparral stands on the campus of California State University, San Marcos. Results from a 1-way ANOVA (F-statistic and degrees of freedom) are shown; $*p < 0.05$, $**p < 0.01$, $***p < 0.001$. Means with a different lower-case letter are significantly ($p < 0.05$) different from each other according to a Tukey-Kramer post-hoc test.

increase over time as litter and soil C and N pools accumulate over the course of succession (Hart et al., 2005; Sinsabaugh et al., 2008; Moya et al., 2018; Ribeiro-Kumara et al., 2020), but the low microbial activity in the NAT stand is still apparent after 5 years of succession even though woody and herbaceous vegetation cover are similar to unburned chaparral values. Peroxidase activity was also significantly lower in the NAT stand, but not correlated with soil C and N like the other enzymes (Fig. 9a; Supplemental Fig. S1). The lack of a significant correlation between peroxidase and soil C has been seen at the global scale (Sinsabaugh et al., 2008), and because peroxidase is involved with lignin degradation (Sinsabaugh et al., 1991), it is possible that C quality (i.e., lignin content) is a better predicator of peroxidase activity that C quantity. As mentioned above, because fungi are primarily responsible with the degradation of lignin-rich organic substrates (Rutigliano et al.,

2007; Sinsabaugh et al., 2008; Dooley and Treseder, 2012; Pressler et al., 2018), it is possible that the lower peroxidase activity in the NAT site is due to lower fungal abundance and/or activity.

4.2. Effects of post-fire management

We also hypothesized that hydroseeding would cause significant changes in microbial abundance and activity because hydroseeding alters soil properties and plant recovery (Vourlitis et al., 2017). Differences in total soil C and N and microbial C between HYD and UNB stands were not statistically significant presumably because of the C input associated with the hydroseed matrix (Zink and Allen, 1998; Garcia-Palacios et al., 2010; Oliveira et al., 2014; Busnardo et al., 2017). The matrix consisted of wood fiber and SpecTack, which added an additional
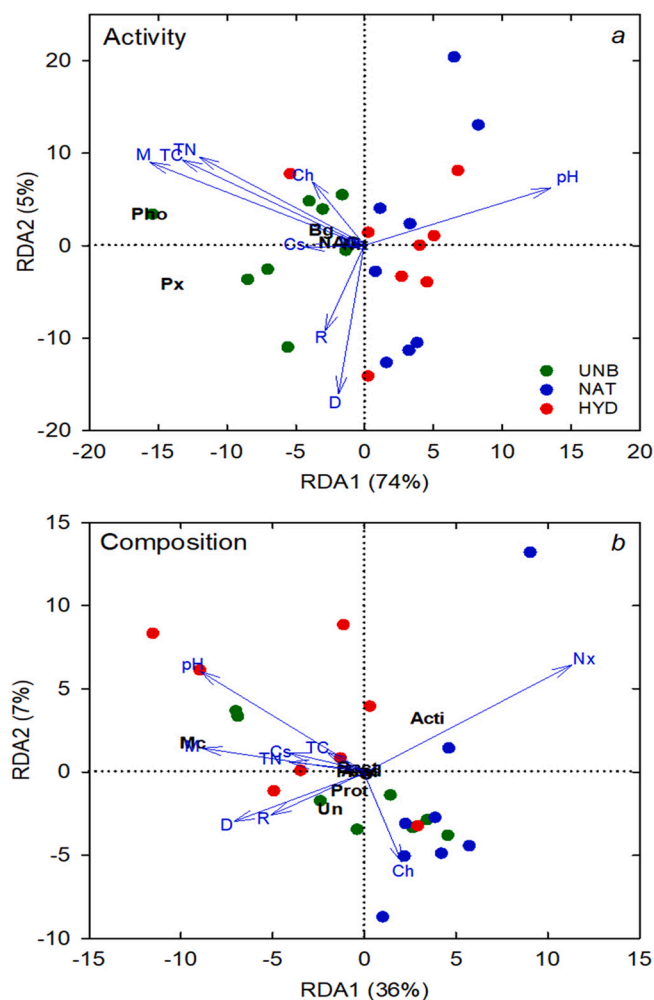
Fig. 9. Redundancy analysis (RDA) results for microbial activity (a) and taxonomic composition (b) for unburned (UNB; green symbols), naturally regenerating (NAT; blue symbols), and hydroseeded (HYD; red symbols) plots. Vectors (blue symbols and arrows) indicate the influence of soil and vegetation variables on the activity scores. Activity scores (a) Mc = Microbial C; Bg = β-glucosidase; Nag = NAGase; Pho = phosphatase; Px = peroxidase. Composition scores (b) Mc = Microbial C; Acid = *Acidobacteria*; Acti = *Actinobacteria*; Bact = *Bacteroidetes*; Firm = *Firmicutes*; Prot = *Proteobacteria*; O = Other; Un = Unclassified. Vectors: M = soil moisture, N_x = extractable N, TN and TC = total soil N and C, respectively, D = shrub density, C_s and C_h = shrub and herbaceous cover, respectively, R = shrub species richness. (For interpretation of the references to colour in this figure legend, the reader is referred to the web version of this article.)

ca. 3400 kg/ha of organic matter, both labile in the form of polysaccharides and recalcitrant in the form of wood fiber, and the presence of the organic matrix was clearly visible on the soil surface even after two years of post-fire recovery. The relatively higher total N in the HYD stand may also have been due to an increase in *Acmispon glaber* (deerweed), which is a legume capable of N_2 fixation (Dorman et al., 2014) that was part of the seed mix and nearly 4-times more-abundant in the HYD than the NAT stand (Supplemental Table S1).

The higher soil C and N in the HYD relative to the NAT stand (Fig. 3c and d) should have caused consistently higher rates of microbial activity in the HYD stand, but only the nitrification rate was higher in the HYD stand. The higher rate of nitrification in the HYD stand was likely due to the increase in total soil C and N, caused by addition of the C-rich matrix and *A. glaber* in the seed mix, and an increase in pH, as the pH of the HYD stand (ca. 7.2) was closer to the pH optimum for nitrification of 7.5–8.0 (Paul and Clark, 2007). However, it is unclear why enzyme activity was

similar in the burned stands given that the HYD stand had higher total C and N and microbial C. Perhaps the increase in pH with hydroseeding acted to reduce enzyme activity (Sinsabaugh et al., 2008). Activities of phosphatase, NAGase, and peroxidase were negatively related to soil pH (Fig. 9a; Supplemental Fig. S1), and the pH optima for glycosidases (β-glycosidase and NAGase) and acid phosphatase are low (ca. pH 5 range) (Sinsabaugh et al., 2008).

Hydroseeding did not significantly affect the relative abundance of bacterial phyla, which was likely due to the high variability in relative abundance within each stand (Fig. 7). One possible reason may be that extractable N appeared to be the biggest driver of microbial C and the relative abundance of *Actinobacteria*, and *Proteobacteria*, but concentrations of extractable N were not significantly different between the stands (Fig. 3b). The only taxon that appeared to be affected by hydroseeding was *Firmicutes* (Fig. 7), which were positively related to soil pH (Fig. 9a; Supplemental Fig. S1).

Interestingly, oligotrophic bacteria (*Acidobacteria, Planctomycetes, Chloroflexi,* and *Verrucomicrobia*) combined only made up between 8 and 14% of all classified bacteria while copiotrophic bacteria (*Proteobacteria, Bacteriodetes, Actinobacteria,* and *Firmicutes*) comprised 50–57% of the classified bacteria (Fig. 7). These results are surprising given that chaparral soils are typically considered to be low in C and nutrients (Jobbagy and Jackson, 2000), which should favor oligotrophic bacteria (Fierer et al., 2007). However, studies of bacterial abundances in other chaparral ecosystems found similar patterns, with copiotrophic bacteria comprising 50–55% of the total soil bacteria in the upper 0–10 cm soil layer (Grant, 2020; Vourlitis et al., 2020). Thus, surface C and N stocks in chaparral appear to be high enough to favor copiotrophic over oligotrophic bacteria. Increases in N availability, which are likely with an increase in nitrification, also favor copitrophic taxa in chaparral (Grant, 2020; Vourlitis et al., 2020).

Vegetation attributes of the stands had no influence on microbial activity or abundance after 5 years of post-fire recovery (Fig. 9a; Supplemental Fig. S1). This is likely due to the fact that vegetation recovery was complete after 5 years of recovery, and differences in stand structure (shrub cover and density and herbaceous cover) were negligible (Figs. 4 and 5). While stand structure was similar between the stands, herbaceous cover was 4–10 fold higher in the HYD than the NAT stand during the first 4 years of succession (Fig. 5b). Furthermore, the HYD stand had higher species richness that the other stands (Fig. 4d), which was due to the additional species added as part of the hydroseed mix (Supplemental Table S1). Thus, in addition to direct C inputs from hydroseeding, differences in herbaceous cover and plant species composition undoubtedly contributed to differences in soil C and N accumulation, microbial C, and microbial activity between the HYD and NAT stands (Hart et al., 2005; Liao et al., 2008; Dooley and Treseder, 2012; Sun et al., 2016).

4.3. Limitations and caveats

Our data suggest that fire can have long-lasting effects on soil C and N stocks and microbial abundance and activity, and that post-fire treatments modify secondary succession in chaparral soil. Unfortunately, the lack of replicated sites limits our ability to generalize beyond the local system; however, our data are broadly consistent with other studies that evaluated the effects of post-fire recovery and management on microbial abundance, composition, and/or activity. Furthermore, our data capture a single period in time, the spring wet season, and omit important temporal variations that occur over seasonal and interannual time scales. Seasonal variations in soil extractable N, pH, and plant cover can be large for both unburned and unburned chaparral (Vourlitis et al., 2021a), which can cause variation in microbial abundance and species composition (Hanan et al., 2016; Grant, 2020; Vourlitis et al., 2020). Changes in vegetation and soil properties during post-fire succession are also large (Hanan et al., 2016; Vourlitis and Hentz, 2016; Vourlitis et al., 2021a, 2021b), especially during the first five years. Vourlitis et al. (2017) found large differences in vegetation cover, soil extractable N,

and microbial biomass between HYD and NAT sites during the first 2 years of post-fire succession and large seasonal variations in many of these variables.

5. Conclusions

Fire and post-fire management in the form of hydroseeding had long-lasting effects on the C and N cycling in a semi-arid chaparral shrubland in southern California. Burned sites had lower soil C and N stocks, which caused a concomitant decline in microbial C and extracellular enzyme activity. The lower soil C stocks for the burned sites could have been due in part to post-fire erosion, as precipitation during the first three years of post-fire recovery was on average 30 mm higher than the average rainfall for the study period, but accumulation of erosional debris was not obvious along the foot of the burned slopes. Furthermore, while hydroseeding effectively eliminated the fire-induced decline in soil C and N, microbial activity (nitrification) and biomass were altered by hydroseeding. This alteration was likely due to the hydroseed matrix, which consisted of C and nutrient inputs, as well as the change in plant species composition due to the artificial seeding. These changes persisted after five years of post-fire recovery even though differences in plant cover and/or species composition between the naturally NAT and HYD strands were no longer statistically significant. This implies initial changes in vegetation from post-fire management can have a long-term impact on soil C and N stocks, and thus bacterial abundance and microbial activity. Given the likely increase in the amount of area burned with climate change (Hurteau et al., 2019), post-fire management strategies such as hydroseeding may become more common. However, hydroseeding must be used with caution because of possible long-term effects on microbial processes and ecosystem C and N cycling and storage.

Declaration of competing interest

The authors declare that they have no known competing financial interests or personal relationships that could have appeared to influence the work reported in this paper.

Appendix A. Supplementary data

Supplementary data to this article can be found online at https://doi.org/10.1016/j.apsoil.2021.104319.

References

Afgan, E., Baker, D., Batut, B., van den Beek, M., Bouvier, D., Čech, M., Chilton, J., Clements, D., Coraor, N., Grüning, B.A., Guerler, A., Hillman-Jackson, J., Hiltemann, S., Jalili, V., Rasche, H., Soranzo, N., Goecks, J., Taylor, J., Nekrutenko, A., Blankenberg, D., 2018. The galaxy platform for accessible, reproducible and collaborative biomedical analyses: 2018 update. Nucleic Acids Res. 46, W537–W544. https://doi.org/10.1093/nar/gky379.

Asche, S.H., Barton, K.P., 1995. Comparison of seedling emergence in hydroseeded and non-hydroseeded burn sites during early stages of post-fire recovery. In: Keeley, J.E., Scott, T. (Eds.), Brushfires in California Wildlands: Ecology and Resource Management. International Association of Wildland Fire, Fairfield, WA, USA, pp. 195–198.

Barcenas-Moreno, G., et al., 2016. Plant community influence on soil microbial response after a wildfire in Sierra Nevada National Park (Spain). Sci. Total Environ. 573, 1265–1274.

Barreiro, A., Martín, A., Carballas, T., Díaz-Ravina, M., 2010. Response of soil microbial communities to fire and fire-fighting chemicals. Sci. Total Environ. 408, 6172–6178.

Barreiro, A., Fontúrbel, M.T., Lombao, A., Martín, A., Vega, J.A., Fernandez, C., Carballas, T., Díaz-Ravina, M., 2015. Using phospholipid fatty acid and community level physiological profiling techniques to characterize soil microbial communities following an experimental fire and different stabilization treatments. Catena 135, 419–429.

Barreiro, A., et al., 2016. Bacterial and fungal growth in burnt acid soils amended with different high C/N mulch materials. Soil Biol. Biochem. 97, 102–111.

Beyers, J., 2004. Postfire seeding for erosion control: effectiveness and impacts on native plant communities. Conserv. Biol. 18, 947–956.

Black, C.H., 1987. Biomass, nitrogen, and phosphorus accumulation over a southern California fire cycle chronosequence. In: Tenhunen, J.D., Catarino, F.M., Lange, O.L., Oechel, W.C. (Eds.), Plant Response to Stress-Functional Analysis in Mediterranean Ecosystems. Springer-Verlag, New York, pp. 445–458.

Bonanomi, G., Ippolito, F., Senatore, M., Cesarano, G., Incerti, G., Saracino, A., Lanzotti, V., Scala, F., Mazzoleni, S., 2016. Water extracts of charred litter cause opposite effects on growth of plants and fungi. Soil Biol. Biochem. 92, 133–141.

Boone, R.D., Grigal, D.F., Sollins, P., Ahrens, R.J., Armstrong, D.E., 1999. Soil sampling, preparation, archiving, and quality control. In: Robertson, G.P., Coleman, D.C., Bledsoe, C.S., Sollins, P. (Eds.), Standard Soil Methods for Long-Term Ecological Research. Oxford University Press, New York, NY, USA, pp. 3–28.

Bowman, R.H., Bishop, R.E., Griffin, R.W., Jones, M.L., 1973. In: Soil Survey of San Diego Area, California. United States Department of Agriculture, Soil Conservation Service, United States Department of Interior, p. 127.

Brookes, P., Kragt, J., Powlson, D., Jenkinson, D., 1985. Chloroform fumigation and the release of soil nitrogen: the effects of fumigation time and temperature. Soil Biol. Biochem. 17, 831–835. https://doi.org/10.1016/0038-0717(85)90143-9.

Busnardo, M.J., McClain, C.D., Schott, K.M., Quinn, M.B., Pollock, M.J., 2017. Techniques to restore coastal scrub at a reclaimed quarry in Central California. Ecol. Restor. 35, 354–361.

Cayan, D.R., Das, T., Pierce, D.W., Barnett, T.P., Tyree, M., Gershunov, A., 2010. Future dryness in the southwest US and the hydrology of the early 21st century drought. Proc. Natl. Acad. Sci. 107, 21271–21276.

Certini, G., 2005. Effects of fire on properties of forest soils: a review. Oecologia 143, 1–10.

Christie, D., 2004. Resampling with excel. Teach. Stat. 26, 9–14.

Cole, J.R., Wang, Q., Fish, J.A., Chai, B., McGarrell, D.M., et al., 2013. Ribosomal database project: data and tools for high throughput rRNA analysis. Nucleic Acids Res. 42, D633–D642. https://doi.org/10.1093/nar/gkt1244.

DeBano, L.F., Conrad, C.E., 1978. The effect of fire on nutrients in a chaparral ecosystem. Ecology 59, 489–497.

Diffenbaugh, N.S., Swain, D.L., Touma, D., 2015. Anthropogenic warming has increased drought risk in California. Proc. Natl. Acad. Sci. 112, 3931–3936. https://doi.org/10.1073/pnas.1422385112.

Dooley, S.R., Treseder, K.K., 2012. The effect of fire on microbial biomass: a meta-analysis of field studies. Biogeochemistry 109, 49–61.

Dorman, H.E., McGlaughlin, M.E., Wallace, L.E., 2014. Widespread variation in NSP1, a gene involved in rhizobium nodulation, across species of acmispon (Fabaceae) from diverse habitats. Botany 92, 571–578. https://doi.org/10.1139/cjb-2014-0039.

Efron, B., Tibshirani, R., 1993. An introduction to the bootstrap. In: Monographs on Statistics and Applied Probability, 57. Springer Science and Business Media, Dordrecht, The Netherlands, p. 436.

Fierer, N., Bradford, B.A., Jackson, R.B., 2007. Toward an ecological classification of soil bacteria. Ecology 88, 1354–1364.

Fontúrbel, M.T., Barreiro, A., Vega, J.A., Martín, A., Jiménez, E., Carballas, T., Fernández, C., Díaz-Raviña, M., 2012. Effects of an experimental fire and post-fire stabilization treatments on soil microbial communities. Geoderma 191, 51–60.

Garcia-Palacios, P., Soliveres, S., Maestre, F.T., Escudero, A., Castillo-Monroy, A.P., Valladares, F., 2010. Dominant plant species modulate responses to hydroseeding, irrigation and fertilization during the restoration of semiarid motorway slopes. Ecol. Eng. 36, 1290–1298.

Grant, T., 2020. MS Thesis. In: Experimental chronic dry atmospheric nitrogen (n) deposition causes a change in soil microbial communities in Southern California semi-arid shrublands. California State University, San Marcos, p. 71.

Hanan, E.J., D'Antonio, C.M., Roberts, D.A., Schimel, J.P., 2016. Factors regulating nitrogen retention during the early stages of recovery from fire in coastal chaparral ecosystems. Ecosystems. https://doi.org/10.1007/s10021-016-9975-0.

Hart, S.C., DeLuca, T.H., Newman, G.S., MacKenzie, M.D., Boyle, S.I., 2005. Post-fire vegetative dynamics as drivers of microbial community structure and function in forest soils. For. Ecol. Manag. 220, 166–184.

Holden, S.R., Rogers, B.M., Treseder, K.K., Randerson, J.T., 2016. Fire severity influences the response of soil microbes to a boreal forest fire. Environ. Res. Lett. 11 (3), 035004 https://doi.org/10.1088/1748-9326/11/3/035004.

Hoover, D.L., Bestelmeyer, B., Grimm, N.B., Huxman, T.E., Reed, S.C., Sala, O., Seastedt, T.R.H., Ferrenberg, S., 2019. Traversing the wasteland: a framework for assessing ecological threats to drylands. Bioscience 70, 35–47. https://doi.org/10.1093/biosci/biz126.

Hubbert, K.R., Wohlgemuth, P.M., Beyers, J.L., 2012. Effects of hydromulch on post-fire erosion and plant recovery in chaparral shrublands of southern California. Int. J. Wildland Fire 21, 155–167.

Hurteau, M.D., Liang, S., Westerling, A.L., Wiedinmyer, C., 2019. Vegetation-fire feedback reduces projected area burned under climate change. Sci. Rep. 9, 2838.

Jackson, C.R., Tyler, H.L., Millar, J.J., 2013. Determination of microbial extracellular enzyme activity in waters, soils, and sediments using high throughput microplate assays. J. Vis. Exp. https://doi.org/10.3791/50399.

Jobbagy, E.G., Jackson, R.B., 2000. The vertical distribution of soil organic carbon and its relation to climate and vegetation. Ecol. Appl. 10, 423–436.

Jonasson, S., 1988. Evaluation of the point intercept method for the estimation of plant biomass. Oikos 52, 101–106.

Kaiser, H.F., 1960. The application of electronic computers to factor analysis. Educ. Psychol. Meas. 20, 141–151.

Kaye, J.P., Romanyà, J., Vallejo, V.R., 2010. Plant and soil carbon accumulation following fire in Mediterranean woodlands in Spain. Oecologia 164, 533–543.

Keeler-Wolf, T., 1995. Post-fire emergency seedling and conservation in southern California shrublands. In: Keeley, J.E., Scott, T. (Eds.), Brushfires in California Wildlands: Ecology and Resource Management. International Association of Wildland Fire, Fairfield, WA, USA, pp. 127–139.

Keeley, J.E., Brennan, T.L., 2012. Fire-driven alien invasion in a fire-adapted ecosystem. Oecologia 169, 1043–1052.

Knelman, J.E., Graham, E.B., Trahan, N.A., Schmidt, S.K., Nemergut, D.R., 2015. Fire severity shapes plant colonization effects on bacterial community structure, microbial biomass, and soil enzyme activity in secondary succession of a burned forest. Soil Biol. Biochem. 90, 161–168.

Knelman, J.E., Graham, E.B., Ferrenberg, S., Lecoeuvre, A., Labrado, A., Darcy, J.L., Nemergut, D.R., Schmidt, S.K., 2017. Rapid shifts in soil nutrients and decomposition enzyme activity in early succession following forest fire. Forests 8, 347. https://doi.org/10.3390/f8090347.

Knicker, H., 2007. How does fire affect the nature and stability of soil organic nitrogen and carbon? A review. Biogeochemistry 85, 91–118.

Lavorel, S., Locatelli, B., Colloff, M.J., Bruley, E., 2020. Co-producing ecosystem services for adapting to climate change. Philos. Trans. R. Soc. B 375, 20190119. https://doi.org/10.1098/rstb.2019.0119.

Liao, C., Peng, R., Luo, Y., Zhou, X., Wu, X., Fang, C., Chen, J., Li, B., 2008. Altered ecosystem carbon and nitrogen cycles by plant invasion: a meta-analysis. New Phytol. 177, 706–714.

Magurran, A.E., 1988. In: . Princeton University Press, Princeton, NJ, p. 179. https://doi.org/10.1007/978-94-015-7358-0.

Marlon, J.R., Bartlein, P.J., Carcaillet, C., Gavin, D.G., Harrison, S.P., Higuera, P.E., Joos, F., Power, M.J., Prentice, I.C., 2008. Climate and human influences on global biomass burning over the past two millennia. Nat. Geosci. https://doi.org/10.1038/ngeo31.

Martí-Roura, M., Casals, P., Romanyà, J., 2011. Temporal changes in soil organic C under Mediterranean shrublands and grasslands: impact of fire and drought. Plant Soil 338, 289–300.

Minnich, R.A., Bahre, C.J., 1995. Wildland fire and chaparral succession along the California-Baja California boundary. Int. J. Wildland Fire 5, 13–24.

Miranda, K.M., Espey, M.G., Wink, D.A., 2001. A rapid, simple, spectrophotometric method for simultaneous detection of nitrate and nitrite. Nitric Oxide 5, 62–71.

Moya, D., González-De Vega, S., García-Orenes, F., Morugán-Coronado, A., Arcenegui, V., Mataix-Solera, J., Lucas-Borja, M.E., Heras, J., 2018. Temporal characterisation of soil-plant natural recovery related to fire severity in burned Pinus halepensis mill. ForestsSci. Total Environ. 640–641, 42–51.

Moya, D., González-De Vega, S., Lozano, E., García-Orenes, F., Mataix-Solera, J., Lucas-Borja, M.E., Heras, J., 2019. The burn severity and plant recovery relationship affects the biological and chemical soil properties of Pinus halepensis Mill. stands in the short and mid-terms after wildfire. J. Environ. Manag. 235, 225–250.

Mulvaney, R.L., 1996. Nitrogen-inorganic forms. In: Sparks, D.L., et al. (Eds.), Methods of Soil Analysis, Part. 3: Chemical Methods. Soil Science Society of America, Madison, WI, pp. 1123–1185.

Nave, L.E., Vance, E.D., Swanston, C.W., Curtis, P.S., 2011. Fire effects on temperate forest soil C and N storage. Ecol. Appl. 21, 1189–1201.

Odion, D.C., Davis, F.W., 2000. Fire, soil heating, and the formation of vegetation patterns in chaparral. Ecol. Monogr. 70, 149–169.

Oliveira, G., Clemente, A., Nunes, A., Correia, O., 2014. Suitability and limitations of native species for seed mixtures to re-vegetate degraded areas. Appl. Veg. Sci. 17, 726–736.

Paul, E.A., Clark, F.E., 2007. In: 3rd ed. Academic Press Inc, Oxford, UK, p. 514.

Pellegrini, A.F.A., et al., 2018. Fire frequency drives decadal changes in soil carbon and nitrogen and ecosystem productivity. Nature 553, 194.

Pressler, Y., Moore, J.C., Cotrufo, M.F., 2018. Belowground community responses to fire: meta-analysis reveals contrasting responses of soil microorganisms and mesofauna. Oikos 00, 1–19. https://doi.org/10.1111/oik.05738.

Quast, C., Pruesse, E., Yilmaz, P., Gerken, J., Schweer, T., Yarza, P., Peplies, J., Glöckner, F.O., 2013. The SILVA ribosomal RNA gene database project: improved data processing and web-based tools. Nucleic Acids Res. 41, D590–D596.

Ribeiro-Kumara, C., Pumpanen, J., Heinonsalo, J., Metslaid, M., Orumaa, A., Jõgiste, K., Berninger, F., Köster, K., 2020. Long-term effects of forest fires on soil greenhouse gas emissions and extracellular enzyme activities in a hemiboreal forest. Sci. Total Environ. 718, 135291.

Running, S.W., 2006. Is global warming causing more, larger wildfires? Science 313, 927–928.

Rutigliano, F.A., De Marco, A., D'Ascoli, R., Castaldi, S., Gentile, A., Virzo De Santo, A., 2007. Impact of fire on fungal abundance and microbial efficiency in C assimilation and mineralisation in a Mediterranean maquis soil. Biol. Fertil. Soils 44, 377–381.

Sawyer, J.O., Keeler-Wolf, T., 1995. In: A manual of California vegetation, p. 471.

Schloss, P.D., Westcott, S.L., Ryabin, T., Hall, J.R., Hartmann, M., Hollister, E.B., Lesniewski, R.A., Oakley, B.B., Parks, D.H., Robinson, C.J., Sahl, J.W., Stres, B., Thallinger, G.G., Van Horn, D.J., Weber, C.F., 2009. Introducing mothur: open-source, platform-independent, community-supported software for describing and comparing microbial communities. Appl. Environ. Microbiol. 75, 7537–7541.

Sims, J.R., Haby, V.A., 1971. Simplified colorimetric determination of soil organic matter. Soil Sci. 112, 137–141.

Sinsabaugh, R.L., Antibus, R.K., Linkins, A.E., 1991. An enzymic approach to the analysis of microbial activity during plant litter decomposition. Agric. Ecosyst. Environ. 34, 43–54.

Sinsabaugh, R.L., Lauber, C.L., Weintraub, M.N., et al., 2008. Stoichiometry of soil enzyme activity at global scale. Ecol. Lett. 11, 1252–1264.

Sun, H., Santalahti, M., Pumpanen, J., Köster, K., Berninger, F., Raffaello, T., Asiegbu, F. O., Heinonsalo, J., 2016. Bacterial community structure and function shift across a northern boreal forest fire chronosequence. Sci. Rep. 6, 324111 https://doi.org/10.1038/srep32411.

Tas, N., Prestat, E., McFarland, J.W., Wickland, K.P., Knight, R., Asefaw Berhe, A., Jorgenson, T., Waldrop, M.P., Jansson, J.K., 2014. Impact of fire on active layer and permafrost microbial communities and metagenomes in an upland Alaskan boreal forest. ISME J. 8, 1904–1919.

Venevsky, S., Thonicke, K., Sitch, S., Cramer, W., 2002. Simulating fire regimes in human-dominated ecosystems: Iberian Peninsula case study. Glob. Chang. Biol. 8, 984–998.

Vourlitis, G.L., Hentz, C.S., 2016. Chronic N addition alters the carbon and nitrogen storage of a post-fire Mediterranean-type shrubland. J. Geophys. Res.Biogeosci. 121, 385–398.

Vourlitis, G.L., Zorba, G., 2007. Nitrogen and carbon mineralization of semi-arid shrubland soil exposed to long-term atmospheric nitrogen deposition. Biol. Fertil. Soils 43, 611–615.

Vourlitis, G.L., DeFotis, C., Kristan, W., 2015. Effects of soil water content, temperature and experimental nitrogen deposition on nitric oxide (NO) efflux from semi-arid shrubland soil. J. Arid Environ. 117, 67–74. https://doi.org/10.1016/j.jaridenv.2015.02.011.

Vourlitis, G.L., Griganavicius, J., Gordon, N., Bloomer, K., Grant, T., Hentz, C., 2017. Hydroseeding increases ecosystem nitrogen retention but inhibits natural vegetation regeneration after two years of chaparral post-fire recovery. Ecol. Eng. 102, 46–54.

Vourlitis, G.L., Grant, T., Sethuraman, A., 2020. Chronic dry nitrogen inputs alter soil microbial abundance of semi-arid shrublands in Southern California. Paper B126-07, American Geophysical Union Fall Annual Meeting, December 16, 2020.

Vourlitis, G.L., Jaureguy, J., Marin, L., Rodriguez, C., 2021. Shoot and root biomass production in semi-arid shrublands exposed to long-term experimental N input. Science of the Total Environment 754, 142204. https://doi.org/10.1016/j.scitotenv.2020.142204.

Vourlitis, G.L., Kirby, K., Vallejo, I., Asaeli, J., Holloway, J.M., 2021b. Potential soil extracellular enzyme activity is altered by long-term experimental nitrogen deposition in semiarid shrublands. Appl. Soil Ecol. 158, 103779.

Wan, S.Q., Hui, D.F., Luo, Y.Q., 2001. Fire effects on nitrogen pools and dynamics in terrestrial ecosystems: a meta-analysis. Ecol. Appl. 11, 1349–1365.

Zink, T.A., Allen, M.F., 1998. The effects of organic amendments on the restoration of a disturbed coastal sage scrub habitat. Restor. Ecol. 6, 52–58.